Mechanical Scope of a Laser Micro-Machined Flexible Substrate

Richard Berenyi
Department of Electronics Technology, Budapest University of Technology and Economics
H-1111 Budapest, Goldmann 3.
E-mail : richard.berenyi@ett.bme.hu

ABSTRACT:

A new 3-D laser micromachining method of 3-D flexible structures has been introduced to enhance the current micromachining technology. The machining is carried out with a simple 2D movement of the laser beam on the work piece. This method can be applied for machining 3-D geometries or bending edges in various materials. The purpose is to extract the material by an ablation of matter in order to achieve "V" shape for multi-bend structure. The process is well controlled and only selective polyimide material removing on bending edges was used. Two-layered polyimide-copper assembly was considered. This is a practical case for multilayer structures such as layered composites and coatings. The mechanical bending analysis of the system with residual stress was carried out with COMSOL Multiphysics. Variations in strain and stress of the structure are demonstrated. Dynamic bending features were also measured and compared to a non laser cut and bended substrate. It's mechanical reliability is improved.

Keywords: micro-machining, 3-D package, laser processing, laser ablation of polyimide, mechanical structures in polyimide, reliability test

INTRODUCTION

As the complexity of electronic systems for portable electronic, aerospace, and military applications increases, more demands are placed on lightweight and compact packaging technologies. To meet these demands, the three-dimensional (3-D) packaging technology is now emerging as a breakthrough of overcoming the limit of two-dimensional (2-D) packages. With its versatility, laser processing by selective ablation of surface patterns can be used to fabricate structures into flexible polymer substrates.

One of the first studies and working high interconnect 3-D System in a Package was that of Chandler N. et al. [1]. solved the 3-D design problem. Another, 3-D-Stacked Integrated Circuit model was employed by IMEC company in 2006, where the connections were realized by micro-vias. Both assemblies were using rigid materials and clumsy 3-D design. In this study, a newly developed 3-D flexible package design and the reliability of the package will be evaluated with a dramatic improvement in compactness resulting in five power chips in a package with lower overall area needs Fig. 1, [2],[3]. Dynamical and normal mechanical stress simulations have been carried out, to prove the necessity of laser micromachining.

3-D PACKAGING WITH BEND-AND-STAY FLEXIBLES

When the composite structure, which is called a flex circuit, is bent, the metal is plastically deformed and gives a mechanical strength to the structure. The objective during bending makes certain that the metal can overwhelm the polymer to hold the final shape. There are two different paths: making the copper thicker may make etching a bit more difficult; it will also take longer to etch and will use more chemistry. On the other hand, reducing the thickness of the polymer in a well-defined, narrow window is used. This bending window generation is a unique application of laser material processing. A bending window can be used to define the exact position of the bending edge as well as the radius and the angle of the deformation [4] [5].

Package in 2D

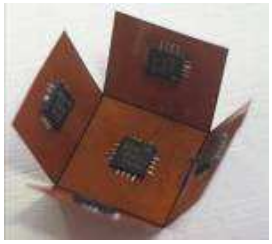

Bending at the edges

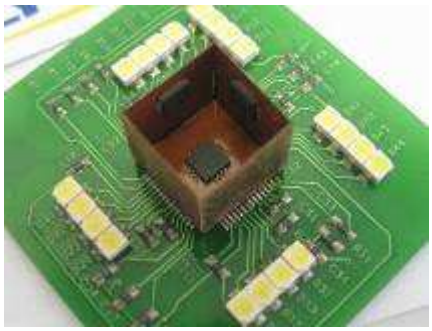

The cube is ready, wires are on the outer side, ICs on the inner side.

Fig. 1: Packaging with Bending the polyimide

MATHEMATICAL DESCRIPTION,

Mathematical equations for mechanical simulations are based on Newton's Law. The equilibrium equations expressed in the stresses for 3-D are (eq. 1, tensorial form in eq.2.) [6][13]:

$$F_x = -\frac{\partial \sigma_x}{\partial x} - \frac{\partial \tau_{xy}}{\partial y} - \frac{\partial \tau_{xz}}{\partial z}$$
$$F_y = -\frac{\partial \tau_{yx}}{\partial x} - \frac{\partial \sigma_y}{\partial y} - \frac{\partial \tau_{yz}}{\partial z} \qquad (1)$$
$$F_z = -\frac{\partial \tau_{zx}}{\partial x} - \frac{\partial \tau_{zy}}{\partial y} - \frac{\partial \sigma_z}{\partial z}$$

$$\sigma_{ij} = \begin{bmatrix} \sigma_x & \tau_{xy} & \tau_{xz} \\ \tau_{yx} & \sigma_y & \tau_{yz} \\ \tau_{zx} & \tau_{zy} & \sigma_z \end{bmatrix} \qquad (2)$$

for 2D the equation can be reduced to:

$$F_x = -\frac{\partial \sigma_x}{\partial x} - \frac{\partial \tau_{xy}}{\partial y}$$
$$F_y = -\frac{\partial \tau_{xy}}{\partial x} - \frac{\partial \sigma_y}{\partial y} \qquad (3)$$

where ***F*** denotes the volume forces (body forces).
Using compact notation, this relationship can be written as:

$$F = -\nabla \sigma \qquad (4)$$

$$\sigma_{ij} = \begin{bmatrix} \sigma_x & \tau_{xy} \\ \tau_{xy} & \sigma_y \end{bmatrix} \qquad (5)$$

where σ is the stress tensor.
The Force in tensorial form:

$$\underline{\underline{F}}_P = (\vec{\rho}_x \circ \vec{i} + \vec{\rho}_y \circ \vec{j} + \vec{\rho}_z \circ \vec{k}) \qquad (6)$$

where $\vec{\rho}_x$, $\vec{\rho}_y$, $\vec{\rho}_z$ are the x, y, z normal vectors in P point.

Stress in Big Bending Deformation

Beam bending is analyzed with the Euler-Bernoulli beam equation. For big deformations the stress in the cross-section is calculated using the formula eq. 7. Fig. 2 shows the deformation during bending. The applied force ***F*** at the ***P*** point deforms the beam with y_p distance causing stress in it [7][8].

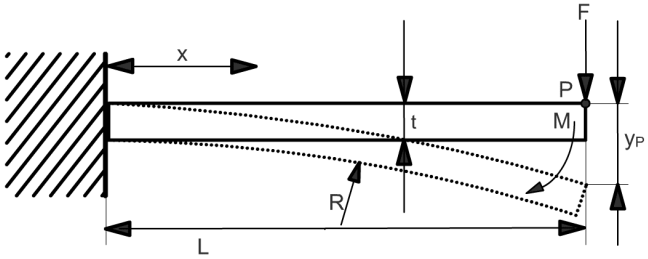

Fig. 2 Bending deformation

$$EI\frac{\partial^2 y}{\partial x^2} = -F(L-x) \qquad (7)$$

after integrations

$$EI \cdot y = -F\left(\frac{Lx^2}{2} - \frac{x^3}{6}\right) \qquad (8)$$

$$y_P = -\frac{F}{EI}\left(\frac{Lx^2}{2} - \frac{x^3}{6}\right) \qquad (9)$$

stress at the function of the distance from the beginning of the beam:

$$\sigma_x = \sigma_x(y) = E\frac{\partial^2 u}{\partial x^2} y_P = \frac{M}{I} y_P \qquad (10)$$

where:
F is the normal force
E is the Elastic modulus
A is the section area
t is the thickness of the beam
M is the bending moment
R is the local bending radius (the radius of bending at the current section)
I is the area moment of inertia
y_A is the position along y axis on the section area in which the stress σ is calculated.

Assumptions must be made:

Assumption of flat sections - before and after deformation the considered section of body remains flat. Shear and normal stresses in this section that are perpendicular to the normal vector of cross section have no influence on normal stresses that are parallel to this section.

The big bending is usually assumed when bending radius 'R' is smaller than ten section thickness t: $R < 10 \cdot t$. In our case R=50-100 µm , t=100 µm.

BENDING WINDOW OPENING BY LASER

In the experiments, a one-sided DuPont Pyralux flexible substrate was involved (FR9150R). The thickness of the insulation layers of the sample was 100 µm).

The material removing process is a simple step-by-step work where the material is removed layer by layer, moving the laser beam in parallel lines. The whole 'V' shape is roughly 40 µm wide (Fig. 3).

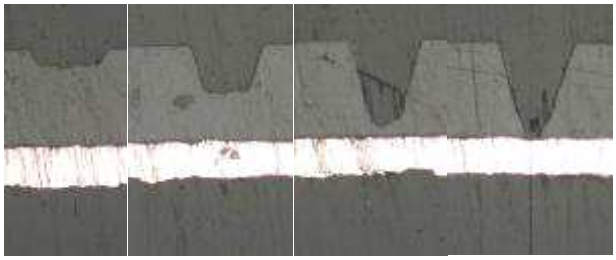

Fig. 3 Cross section of 'V' cut creation steb-by-step

Multilevel laser machining

Investigation on the different geometrical forms of bending windows has proved that the application of a single 'V' form window for 90° bending is not reasonable (Fig. 4).

Fig. 1: Fig. 4 Cu cracks at the edge (bending angle 52°)

Bends over 90° place the greatest stress on formed areas. To decrease the mechanical stress, bending with distributed parameters was used. The bending is not concentrated at one point.

Fig. 5 shows the cross section of multi-shaped bending windows. The 'V' shape's angle and raster can be calculated in the function of the bending radius and the bending angle.

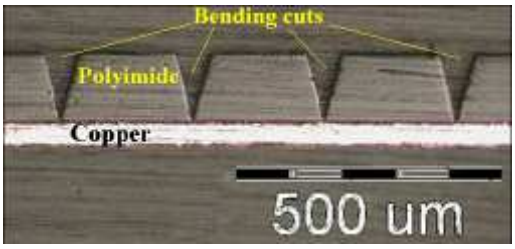

Fig. 5 Polyimide after multilevel machining

Provide the largest bend radius possible

The designer is always advised to provide the largest practical radius through bend areas. For single metal layers, it is about 3–6 times the circuit thickness. This design approach is especially important, not only for dynamic flex, but also in flex applications that are apparently static in nature, for example, bend-and-stay structures. In Fig. 6, the graphic and simple equation illustrates the effect of bend-radius diameter on the copper foil [9].

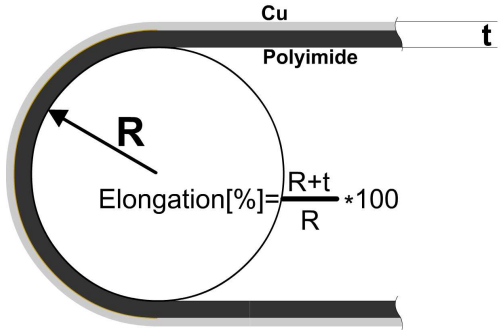

Fig. 6 Equation of elongation

The elongation requirements for the copper foil increase significantly as the bend radii decrease. During the bending procedure, the elongation limit of the material should not be reached to avoid copper breaking. The copper's elongation at break is 40%. Fig. 7 shows the elongation values at different bend radii and substrate thicknesses [10].

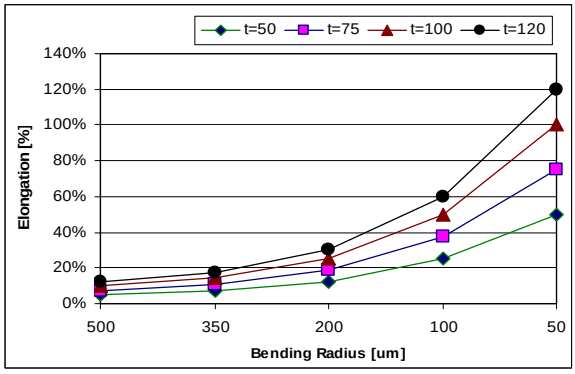

Fig. 7 Elongation vs. bend radius and thickness

Normally, if the bending radius is smaller than 200 µm, it results in more than 40% elongation, which is the limit in copper break. With multilevel bending window formation, the mechanical stress and the elongation have been decreased by distributed bending. As a result, a 180° bended polyimide

substrate is seen in Fig. 8. The bending radius is just about 50 µm, reached with six smaller bending windows (6*30°).

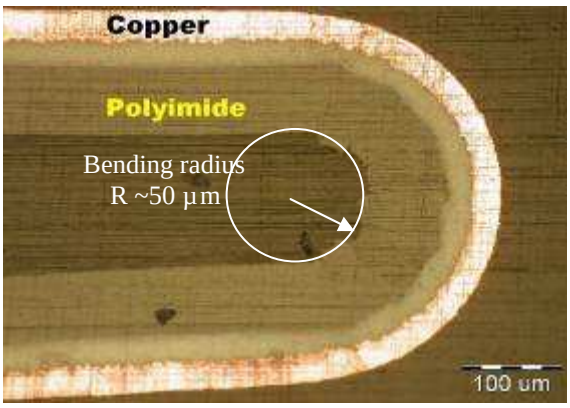

Fig. 8 Polyimide bended at the angle of 180°

EXPERIMENTAL RESULTS

Dynamic Tests

As this radius is small and it is feared that a crack will be formed by the time, we decided to measure its dynamic bending feature (sheet resistance vs. time). For the experiment a test coupon shown in Fig. 9 is the recommended standard specimen pattern for either single- or double sided flexible printed wiring [12]. The sheet resistance of the copper was continuously measured and logged by computer.

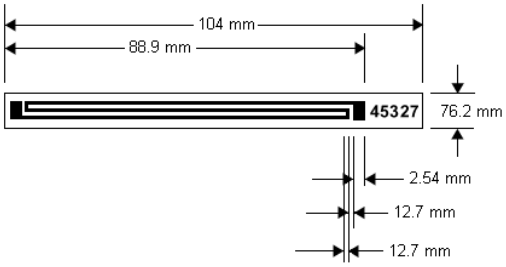

Fig. 9. Bending-test piece.

Copper break was noticed by increasing in resistance. At this moment the bending test cycles have been aborted, and the number of cycles has been registered.

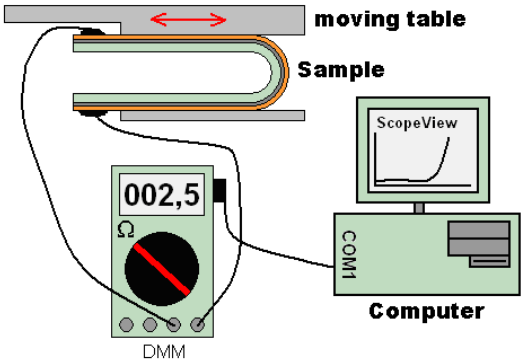

Fig. 10 Measuring structure

The new form was compared to a non laser cut and bended substrate, Fig. 11. As it can be seen in the graphs the dynamic mechanical property of the polyimide hasn't fallen off, on the contrary the mechanical reliability is improved. The laser micro-machined polyimide could stand 6 times more moving cycle than the original polyimide.

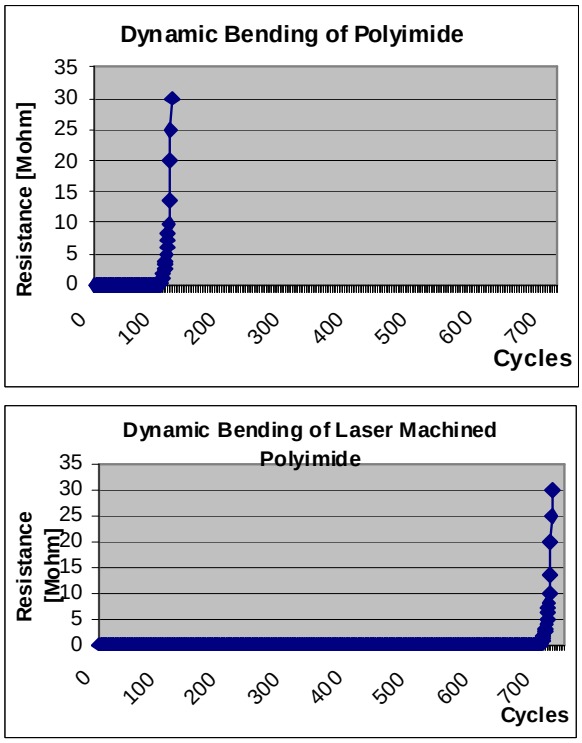

Fig. 11 Dynamic bending of Polyimide

Mechanical Stress Simulation

A mechanical bending analysis was carried out in a two layered, polyimide + copper substrate. The "F" force represents the distributed load, which bends the system (Fig. 12).

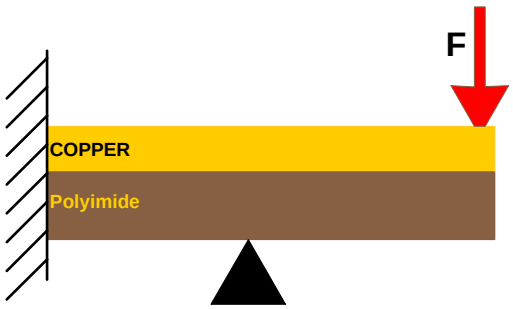

Fig. 12 Bending model

The Graphical simulation results can be seen in Fig. 14 while the numerical results are in Fig. 15. The maximum Stress marked with white colour, and its value is $5 \cdot 10^9$ Pa During the simulation the following material properties were used (Table 1) [10][11].

Table 1. Material properties

	Kapton	**Copper**
Material model	Isotropic	Isotropic
Young Modulus [GPa]	3,1	120
Poisson ration	0,33	0,34
Thermal Expansion [1/K]	$1{,}2\cdot10^{-5}$	$16{,}5\cdot10^{-6}$
Density [kg/m^3]	1300	8960
Thickness [μm]	100	30

The simulation uses boundary conditions like fixed (eq. 11), free end (eq. 12), force contact point (eq. 13). Fig. 13 shows the coordinates (u, w) calculated continuously [13][14].

$$u\big|_{x=0} = 0\,,\ \frac{\partial u}{\partial x}\Big|_{x=0} = 0 \qquad (11)$$

$$\frac{\partial^2 u}{\partial x^2}\Big|_{x=L} = 0\,,\ \frac{\partial^3 u}{\partial x^3}\Big|_{x=L} = 0 \qquad (12)$$

$$-\frac{\partial}{\partial x}\left(EI\frac{\partial^2 u}{\partial x^2}\right) = F \qquad (13)$$

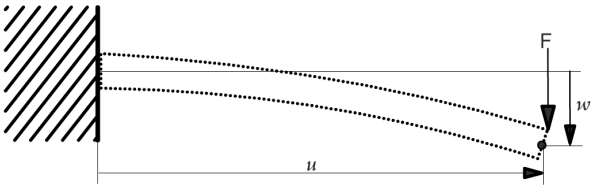

Fig. 13 Calculated coordinates

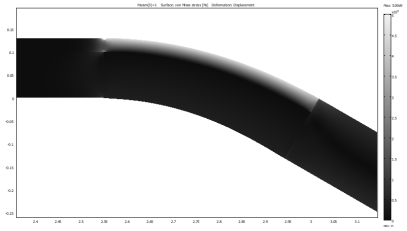

$\sigma = 5{,}1\cdot10^9$

No bending edge

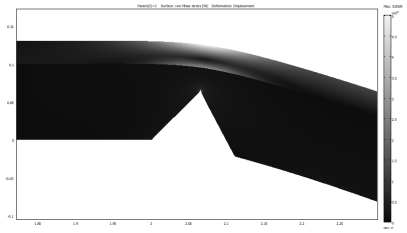

$\sigma = 4{,}6\cdot10^9$

One bending edge

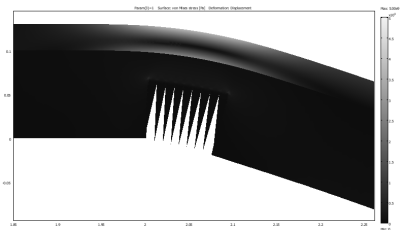

$\sigma = 4{,}13\cdot10^9$

10 pieces of bending edges

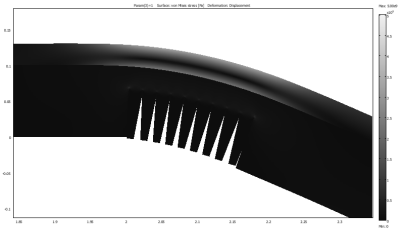

$\sigma = 3{,}28\cdot10^9$

10 pieces of bending edges with gap

Fig. 14 Graphical results of bending simulation

The simulation is proved the need of laser cuts for bending edges. Comparing the result to the polyimide without bending edges the mechanical stress is decreased by the number of laser cuts. An other positive effect of the gap can be observed in Fig. 15. As 10 μm gap have left between laser cuts the bending stress is reduced by 20%.

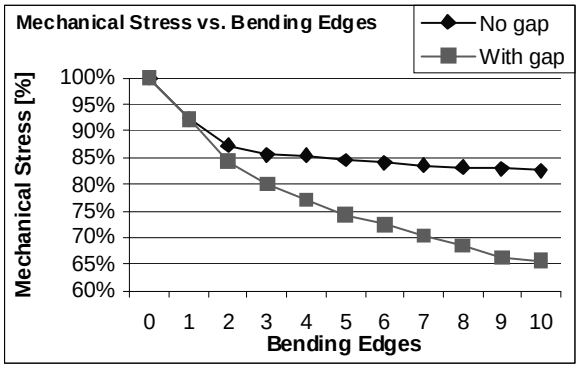

Fig. 15. Numerical results of bending simulation. Maximum values of stress are marked.

CONCLUSION

As the result of our experiments we can state that laser processing of polymeric materials using optimum processing parameters has proved to be an efficient tool for micro-machining.

Most of the polyimide substrates can be processed and high-resolution patterns can be generated by laser. The polyimide layer was ablated to fabricate 'V' form bending windows at 30°, 90°, 180° and the copper leads were not damaged.

The dynamical stress test proved the processed polyimide is 6 times better for dynamic bending in small radius.

The simulation is proved the need of laser cuts for bending edges. The mechanical stress is decreased by the number of laser cuts and the effect of the gap is also positive. A 10 μm gap reduced the bending stress by 20%.

This technology is very likely to be applicable for creating 3-D configuration with today's emphasis on micropackaging likely to intensify, the benefits of designing with flex circuitry become more appealing than ever.

REFERENCES

[1] Faure C., Val A., Couderc P., Chandler N., Preziosi E., Ousten Y., Levrier B.: 3-D System-in-Package : Technology Improvements for Volume Manufacturing. IMAPS MicroTech 2006, Cambridge, 7-8 March 2006

[2] Chou B., Solomon B., Hunt J.: Ultra-High Denisty Interconnect Flex Substrates. High Density Interconnect, December, 1998. pp.14-21.

[3] Minari N., Tadashi K., Yoshihiro O.: A Novel Localizable HDI-PWB Solution. High Density Interconnect, vol.3 (2000), no.12, pp.20-25.

[4] Bityurin N., Luk'yanchuk B.S., Hong M.H., Chong T.C.: Models for laser ablation of polymers. Chemical Reviews vol.103 (2003), pp.519-552.

[5] Duley W.W.: UV Lasers Effects and Applications in Material Science. Cambridge University Press, Cambridge, 1996.

[6] Chung T.J. : General Continuum Mechanics, Cambridge University Press, 2007.

[7] Witmer E.A.,: Elementary Bernoulli-Euler Beam Theory. MIT Unified Engineering Course Notes: pp. 5-114, 1992.

[8] Shigley J, Mechanical Engineering Design, McGraw Hill, 1986, ISBN 0-07-100292-8

[9] Fjelstad J. : Flexible Circuit Technology, Atlantic Books, 2006, ISBN 0-9667075-0-8

[10] Mechanical properties of annealed copper from MatWeb. http://www.matweb.com/

[11] Mechanical properties of Kapton polyimide from MatWeb. http://www.matweb.com/

[12] Flexural Fatigue and Ductility, Flexible Printed Wiring, IPC-TM- 650 Standard No. 2.4.3.1.

[13] Pepper W.D., Heinrich J.C., : The Finite Element Method. Taylor & Francis, New York, 2006.

[14] Zimmerman W.B. : Multiphysics Modelling with Finite Element Methods, Word Scientific, Singapore, 2008.